Discovering heavy neutral leptons with the Higgs boson

Nicolás Bernal,[*] Kuldeep Deka,[†] and Marta Losada[‡]
New York University Abu Dhabi, PO Box 129188, Saadiyat Island, Abu Dhabi, United Arab Emirates

(Received 24 January 2024; accepted 14 August 2024; published 4 September 2024)

We study the dominant signatures that arise in Higgs physics at colliders when extending the Standard Model (SM) with a Yukawa interaction to heavy neutral leptons, while suppressing their mixing to active neutrinos. We focus on the production of heavy neutral leptons from Higgs bosons that subsequently decay via the Higgs to SM fermions to determine the experimental reach at the LHC detectors and far detectors such as FASER and MATHUSLA. We also determine the impact of precision Higgs constraints on beyond-SM parameters in this scenario.

DOI: 10.1103/PhysRevD.110.055011

I. INTRODUCTION

The discovery of the Higgs boson in 2012 [1,2] vindicated the Standard Model (SM) to an unprecedented level of accuracy. The myriad of successes of the SM over the years include, but are not limited to, the discovery of gluons [3], the prediction of $W^{\pm}/Z^0$ bosons and their masses [4], and the prediction of charm/top quarks [5–7]. These successes are, however, somewhat shadowed due to a few shortcomings that persist till date, among which neutrino mass, dark matter, matter-antimatter asymmetry, and a few anomalies in the experimental observables are the most vexing ones. There is a plethora of beyond-SM scenarios that have been proposed to address these shortcomings. The way forward now is to meaningfully constrain these scenarios through precision Higgs-physics observables, be it at the HL-LHC or future Higgs factories.

Following the confirmation of neutrino masses through neutrino oscillation experiments, a natural question arises regarding whether they are somehow linked to the Higgs mechanism, which imparts mass to all other elementary particles through the electroweak symmetry breaking. One plausible extension of the SM to address this inquiry involves the introduction of heavy neutral leptons (HNLs). These sterile neutrinos, being singlets under the SM gauge group, interact with the Higgs boson and active SM neutrinos through Yukawa interactions. Moreover, depending on the model, they can undergo mixing with SM neutrinos following the electroweak phase transition, once the Higgs acquires a vacuum expectation value (vev). For detailed reviews, see Refs. [8,9]. Nonzero neutrino masses can be realized through various types of mechanisms, popular among which include seesaw, scotogenic, etc. [10–19]. Apart from the generation of neutrino masses, these HNLs can also help in the dynamical generation of the baryon asymmetry of the universe via leptogenesis [20–25] and may even be a viable candidate for explaining the observed dark-matter relic abundance [26–28]. Interestingly, all three of these problems can be solved within the framework of neutrino minimal SM by the introduction of three HNLs [22,29].

However, instead of focusing on particular models, here we follow a model-independent approach and study collider experimental tests of HNLs. Many experimental searches have focused on the high-mass regime, where HNLs are produced directly or in some prompt decay channels [30–36], with numerous dedicated analyzes, for example, in Refs. [37–58].

Another possibility occurs in the parameter space where HNLs can decay with a sizable displacement in LHC detectors, featuring a displaced vertex that is a distinctive signature of their existence [59]. Recently, several studies have promoted the use of these types of dedicated LHC searches for HNL with associated charged leptons [60–70], from Higgs decays [71–77], or for LHCb [78]. There is also a potential to search for such signatures at DUNE [79,80], IceCube [81], future lepton colliders [82,83] and SHiP [84,85], the latter expected to greatly improve the sensitivity to HNL below the c-quark mass, with HNLs abundantly produced by meson decays [86]. CMS and ATLAS have already performed some of such analyzes through various channels [87–91].

In the same spirit, several specific far detectors have been proposed at the LHC, with the aim of detecting long-lived particles, including FASER [92,93],

[*]Contact author: nicolas.bernal@nyu.edu
[†]Contact author: kuldeep.deka@nyu.edu
[‡]Contact author: marta.losada@nyu.edu

MoEDAL-MAPP [94,95], MATHUSLA [96–98], ANUBIS [99], CODEX-b [100], and FACET [101]. Among them, FASER and MoEDAL-MAPP are already in operation, and others are still in discussion. The particular scenario where HNLs are long-lived particles has been extensively discussed in the recent literature [102–111].

It is important to note that all analyses conducted so far have focused on the search for HNLs through their mixing with SM active neutrinos. However, the presence of significant mixing and the production/decay of HNLs via this mixing highly depends on the model and are not always guaranteed. As discussed in the Appendix, there could be scenarios where the Yukawa interactions dominate and contribute solely to the HNL phenomenology. Therefore, as an alternative to the conventional approach, we propose a novel and complementary method that exploits their Yukawa coupling to the SM Higgs boson. We adopt a cautious stance and treat Yukawa couplings and mixing angles as independent parameters to avoid assumptions. For simplicity and as an initial step, we assume that all mixing angles are very small, focusing on the role of trilinear Yukawa couplings. This approach could also provide information on the Higgs mechanism and the electroweak symmetry breaking.

The paper is structured as follows. In Sec. II, the model and the setup of the analysis are presented. Then, in Sec. III, the production and decay modes of HNLs through Higgs interactions are described, together with the constraints from precision Higgs measurements. Sections IV–VI are devoted to the analysis of searches for HNLs that decay promptly, produce a displaced vertex, or decay in far detectors, respectively. Finally, we conclude in Sec. VII.

II. SETUP

In this work, we extend the SM by introducing n HNLs denoted as $\tilde{N}$, which could be Dirac or Majorana particles. The relevant Yukawa interaction term is expressed as $y_{N\alpha}\bar{\tilde{N}}\tilde{H}^\dagger L_\alpha$, where H represents the SM Higgs doublet, $\tilde{H} \equiv i\sigma^2 H^*$ (with σ^2 being the second Pauli spin matrix), L_α are the SM lepton doublets for $\alpha = e, \mu, \tau$, and $y_{N\alpha}$ are the Yukawa couplings between the HNLs and the SM leptons. We denote the mass of the HNL as m_N, without explicitly writing the mass term, as it differs slightly depending on whether $\tilde{N}$ is a Dirac or Majorana particle.

Following electroweak symmetry breaking, the Higgs field acquires a vacuum expectation value $v_h \simeq 246$ GeV, leading to Yukawa interactions generating Dirac masslike terms $(M_D)_{N\alpha} \equiv y_{N\alpha} v_h/\sqrt{2}$. Similar terms can also arise if additional scalar fields are present in the model, which also acquire vevs. The physical mass eigenstates for the three SM neutrinos ν and the n HNLs are determined by diagonalizing the full mass matrix specific to the model. To fit neutrino oscillation data, at least $n \geq 2$ HNLs are required [112,113]. Looking to accommodate sub-eV neutrino masses [114] imposes constraints on the parameter space of the model. The diagonalization to the mass basis could also cause mixings between HNLs and SM neutrinos. If present, then the mixings result in HNLs inheriting interactions with other SM particles, especially the $W^\pm$ and Z bosons. For a type-I seesaw mechanism [10–16], the mixing scales as $y_{N\alpha} v_h/m_N$. However, in inverse seesaw and double-seesaw models [115,116], the mixing contributions can be smaller due to the presence of an additional mass scale. There are also cases where the mixing contributions can be tuned to be precisely zero [117,118], as explicitly discussed in the Appendix. Overall, it is important to emphasize that, while there are well-motivated models linking Yukawa couplings and mixing angles, these relations should not be assumed to hold universally.

For an agnostic perspective, free from specific model assumptions, we consider Yukawa couplings and mixing angles as independent parameters. As a first step, we focus on a single HNL and its production and decay through interactions with the Higgs boson, assuming negligible mixing with the SM neutrinos, resulting in minimal coupling of HNLs to W and Z bosons.[1]

III. PRODUCTION AND DECAYS OF HNLS

In this work, we consider the production of HNLs through the decay of the Higgs boson, which implies that m_N has to be in the GeV ballpark. Much heavier particles could not be kinematically produced by Higgs decays; lighter HNLs, below a few GeVs, are mainly produced by meson decays [119].

For the following phenomenological analysis, we have used a modified version of the FeynRules [120,121] model HeavyN [40,44,49], with a single HNL and only Yukawa couplings. Signal and background events are generated using MadGraph5_aMC@NLO v2.9.16 [122,123] interfaced with PYTHIA 8 [124] for parton showering and fragmentation. The events are then passed through DELPHES 3.5 [125] in order to implement detector effects and various reconstruction algorithms.

A. Production of HNLs

Here we consider the production of HNLs through Higgs decays. At the LHC, Higgs bosons are produced mainly by the gluon-gluon fusion mechanism (ggF) mediated by triangular loops of heavy quarks, with a cross section $\sigma_{\text{ggF}} \simeq 54.8$ pb at $\sqrt{s} = 14$ TeV [126]. The second most important channel corresponds to vector-boson fusion (VBF), with a cross section $\sigma_{\text{VBF}} \simeq 4.26$ pb also at $\sqrt{s} = 14$ TeV [127]. Other channels such as the associated

[1]For example, with zero mixings at tree level, $W \to N\ell$ can still arise at one loop through a virtual Higgs, but is suppressed by the loop factor and the square of the Yukawa of the lepton.

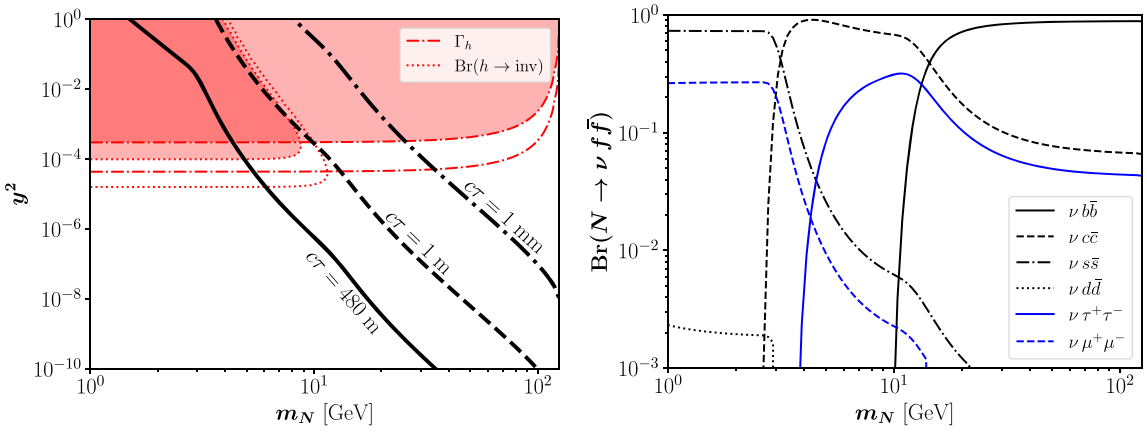

FIG. 1. Left: contours for the HNL decay lengths $c\tau = 1$ mm, 1 m, and 480 m. The red areas are in tension with the invisible decay of the Higgs or its total decay width, whereas the red dotted and dashed dotted lines correspond to projected sensitivities at HL-LHC. Right: branching ratios for the three-body decay of the HNL, summing over all neutrino flavors.

production with massive gauge bosons or heavy-quark pairs are further suppressed [128].

The partial decay width of the Higgs boson into a HNL and an active neutrino is given by

$$\Gamma(h \to N\nu) = \frac{y^2}{8\pi} m_h \left[1 - \left(\frac{m_N}{m_h}\right)^2\right]^2, \tag{3.1}$$

where $m_h \simeq 125$ GeV is the Higgs mass. It is interesting to note that the neutrino flavor ν_α depends on the Yukawa $y_{N\alpha}$. However, since the LHC is insensitive to this flavor, the coupling y appearing in Eq. (3.1) must be understood as the sum of all Yukawa couplings, that is, $y^2 \equiv y_{Ne}^2 + y_{N\mu}^2 + y_{N\tau}^2$. This new decay mode contributes to the total decay width of the Higgs, which in the SM is $\Gamma_h \simeq 4.1$ MeV [129], and has been measured at the LHC to be $\Gamma_h = 3.2^{+2.4}_{-1.7}$ MeV [130]. HL-LHC is expected to improve this measurement to a precision of 5.3% [131]. In the left panel of Fig. 1, the red dashed dotted region labeled Γ_h shows the parameter space in tension with measurements of the Higgs total decay width and projections for HL-LHC.

B. Decays of HNLs

In the present scenario, HNLs can only decay to an active neutrino and an off-shell Higgs that later decays to a fermion-antifermion pair. Away from kinematical thresholds, each individual partial decay width scales as

$$\Gamma(N \to \nu f\bar{f}) \propto y^2 \frac{m_f^2 m_N^5}{m_h^6}, \tag{3.2}$$

where m_f corresponds to the mass of the fermion f. Furthermore, due to the mass hierarchy, the total decay width is dominated by the contribution of s quarks ($1\,\text{GeV} < m_N \lesssim 3\,\text{GeV}$), c quarks ($3\,\text{GeV} \lesssim m_N \lesssim 15\,\text{GeV}$), or b quarks ($15\,\text{GeV} \lesssim m_N < 125\,\text{GeV}$), with corresponding branching fractions Br($N \to \nu f\bar{f}$) shown in the right panel of Fig. 1. It is interesting to note that the branching fractions depend only on m_N (and not on y), as the flavor of the active neutrino is not measurable at the LHC. Furthermore, the lifetime of HNLs can span a wide range and therefore can have prompt decays ($c\tau \lesssim 1$ mm), displaced decays [$\mathcal{O}(1)$ mm $\lesssim c\tau \lesssim \mathcal{O}(1)$ m], or even decays outside of the ATLAS or CMS detectors [$\mathcal{O}(1)$ m $\lesssim c\tau$], where $c\tau$ corresponds to the decay length. Additionally, if $c\tau \sim \mathcal{O}(100)$ m, HNLs can decay in far detectors such as FASER or MATHUSLA. The left panel of Fig. 1 shows contours with thick black lines for $c\tau$ in the plane $[m_N, y^2]$.

It is interesting to note that in our framework the Higgs boson does not have any additional invisible decay mode.[2] However, one can still have an effective contribution to its invisible decay, if the HNL decays outside the detector. The probability of a HNL to decay outside the detector is given by

$$\mathcal{P} = \frac{1}{\mathcal{N}_{\text{ev}}} \sum_{i=1}^{\mathcal{N}_{\text{ev}}} \Theta(d_{xy}^{(i)} - L_{xy}) \Theta(d_z^{(i)} - L_z) \tag{3.3}$$

with Θ being the Heaviside step function,

$$d_{xy}^{(i)} = c\tau \frac{\sqrt{(p_x^{(i)})^2 + (p_y^{(i)})^2}}{m_N}, \tag{3.4}$$

$$d_z^{(i)} = c\tau \frac{|p_z^{(i)}|}{m_N}, \tag{3.5}$$

[2]In the SM, the main invisible decay mode of the Higgs corresponds to $h \to ZZ^* \to 4\nu$, with a branching fraction ~0.1% [130]. The decay $h \to N\nu$ with $N \to \nu\nu\nu$ can only occur through the mediation of a Z boson, and therefore it is not present in our scenario where the mixing angles are zero.

are the transversal and the longitudinal decay lengths in the laboratory frame, and (p_x, p_y, p_z) the 3-momentum of the HNL, for a large number of events $\mathcal{N}_{\rm ev}$. Therefore, the corresponding Higgs boson invisible decay branching ratio $\mathrm{Br}(h \to \mathrm{inv})$ is given by

$$\mathrm{Br}(h \to \mathrm{inv}) = \frac{\mathcal{P}\Gamma(h \to N\nu)}{\Gamma(h \to N\nu) + \Gamma_h}, \tag{3.6}$$

and has being measured by the ATLAS collaboration to be $\mathrm{Br}(h \to \mathrm{inv}) < 10.7\%$ [132] and the CMS collaboration $\mathrm{Br}(h \to \mathrm{inv}) < 15\%$ [133] at 95% CL. Furthermore, future measurements at the HL-LHC are expected to strengthen this bound to $\mathrm{Br}(h \to \mathrm{inv}) \lesssim 1.9\%$ [134]. The physical dimensions of the ATLAS detector are about $L_{xy} \simeq 11$ m in radius and $2L_z \simeq 44$ m in length, up to the muon spectrometer [135]. In the left panel of Fig. 1, the red dotted region labeled $\mathrm{Br}(h \to \mathrm{inv})$ shows the parameter space in tension with the constraint from the invisible decay of the Higgs and projections for HL-LHC.

IV. PROMPT DECAYS

In this section, we first look at single Higgs bosons produced through VBF in the quest for reducing the background by exploiting the characteristic features of its two hard forward jets. We will use an integrated luminosity $\mathcal{L} = 3$ ab^{-1} and a center-of-mass energy $\sqrt{s} = 14$ TeV.

VBF has a very peculiar topology, with two leading jets (j_1 and j_2) typically present in the forward region and reside in opposite hemispheres of the detector. This results in a large pseudorapidity separation $\Delta\eta_{j_1 j_2}$ and a large invariant mass $m_{j_1 j_2}$. The Higgs boson resulting from VBF also tends to have a significant transverse momentum p_T, which requires that the azimuthal separation between the two leading jets $\Delta\phi_{j_1 j_2}$ be small. This is in contrast to what is expected for QCD multijet events and hence can be used as a strategy to suppress such large backgrounds. The Higgs particle then decays to a HNL and a SM neutrino, given by Eq. (3.1). The HNL can then further decay to a pair of $b\bar{b}$ and an active SM neutrino mediated by an off-shell Higgs. As shown in the right panel of Fig. 1, above the $b\bar{b}$ mass threshold, this channel has the highest branching ratio. The main background that contributes to this process is the SM VBF Higgs production itself, where the Higgs decays subsequently to a $b\bar{b}$ pair. The ggF process for Higgs production, with the Higgs decaying to $b\bar{b}$, is also an important background to consider. Although the ggF event topology is very different from that of VBF, there is a nonvanishing probability of the two initial gluons radiating off two hard forward jets that mimic the VBF topology. The effect is enhanced by the fact that the production cross section of ggF is one order of magnitude higher than that of VBF. This non-negligible contribution also motivated in our study the inclusion of the ggF production channel into the signal events of the process we are interested in.

Among other backgrounds, the $t\bar{t}$ + jets case is important because of the automatic presence of two b jets along with other light jets that could mimic the two forward jets in VBF. The cross section is also quite large (990 pb at next-to-next to LO [136]) compared to the VBF and ggF processes. Additionally, $b\bar{b}$ + jets with its huge cross section ($\sim 10^5$ pb [137]) can also be relevant if the associated jets are in the forward region.

Initial- and final-state radiation in VBF processes can also result in additional jets. Specific requirements on such jets also help to remove QCD multijet backgrounds, including $t\bar{t}$ + jets. One such metric used to examine whether a subleading jet can be associated with having been emitted from either of the two primary leading jets in the context of a VBF process is the comparison between the invariant mass of the subleading jet and one of the two primary leading jets. This comparison is made with respect to the invariant mass $m_{j_1 j_2}$. Specifically, it checks whether the invariant mass of the subleading jet j_i (with $i \geq 3$) and that of one of the two leading jets is smaller compared to $m_{j_1 j_2}$, and is given by

$$m_{j_i}^{\rm rel} \equiv \frac{\min(m_{j_1 j_i}, m_{j_2 j_i})}{m_{j_1 j_2}}. \tag{4.1}$$

Small values of $m_{j_i}^{\rm rel}$ indicate that the additional jet is compatible with the final-state radiation.

Finally, the two b quarks arising from the HNL decay are expected to carry an invariant mass closer to the actual HNL mass. Although the entire HNL mass cannot be resolved due to the presence of two different sources of missing transverse energy $\not{E}_T$ (i.e., the two active neutrinos in the final state), a cut on the invariant mass of the two b quarks around the HNL mass still gives some handle to reduce the SM VBF, ggF, and $t\bar{t}$ + jets backgrounds. A cut on the maximum ΔR of the two b jets helps to further reduce the $t\bar{t}$ + jets and SM-ggF background events, as their associated b jets tend to have a larger separation.[3] The two upper plots of Fig. 2 show the distributions for the invariant mass $m_{b_1 b_2}$ and the separation $\Delta R_{b_1 b_2}$ of the two b-tagged jets for the signal corresponding to $m_N = 65$ GeV (thick black lines) and the four SM background processes discussed (thin colored lines). As already discussed, the two neutrinos in the final state result in a substantial amount of missing energy, as shown in the lower plot of Fig. 2.

Taking cues from the behavior of the signal and backgrounds, we employ the following selection criteria:

S1: We demand that the event contains no charged lepton candidates nor photons.

[3] ΔR denotes the distance in the pseudorapidity-azimuth plane, namely $\Delta R \equiv \sqrt{(\Delta\eta)^2 + (\Delta\phi)^2}$.

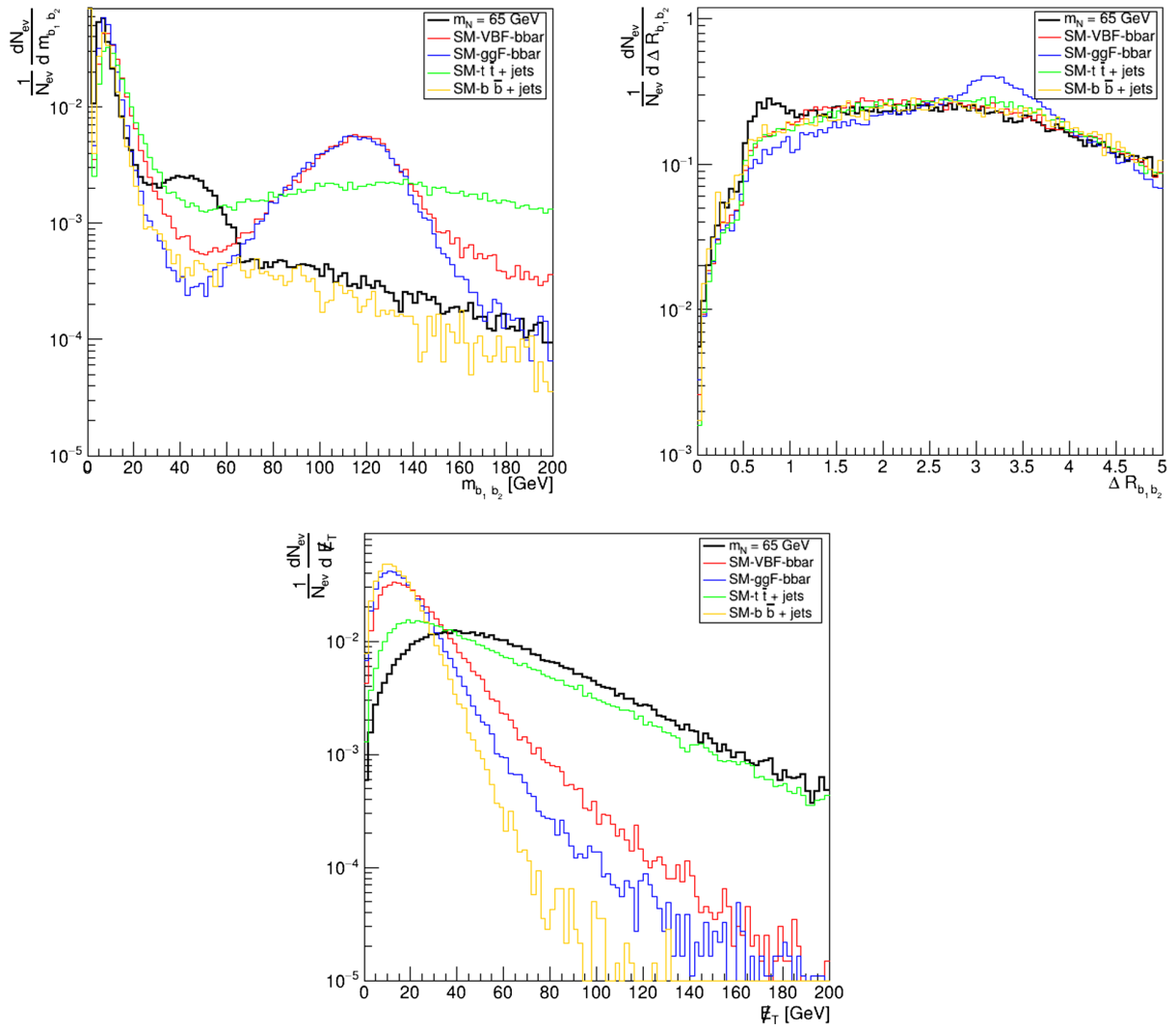

FIG. 2. Kinematic distributions for the invariant mass $m_{b_1 b_2}$ and the separation $\Delta R_{b_1 b_2}$ of the two b-tagged jets, and the missing transverse energy $\not{E}_T$, for $m_N = 65$ GeV.

S2: We require at least two jets that are not b tagged and at least two b-tagged jets.

S3: We want the two leading non-b jets to satisfy $p_{T_{j_1}} > 60$ GeV and $p_{T_{j_2}} > 40$ GeV. We also want the total scalar sum of all non-b jets to be $H_T > 140$ GeV.

S4: Among the observables derived from the two leading non-b jets, we demand that they follow the VBF topology by requiring them to be in opposite longitudinal hemispheres ($\eta_{j_1} \times \eta_{j_2} < 0$), to have a large pseudorapidity separation ($\Delta\eta_{j_1 j_2} > 3.5$) and a large

TABLE I. Cut flow of fraction of surviving events for $m_N = 65$ GeV.

	Signal		Backgrounds			
Cut flow	VBF	ggF	SM-VBF	SM-ggF	$t\bar{t}+$ jets	$b\bar{b}+$ jets
S_1 and S_2	5.96×10^{-2}	1.24×10^{-2}	0.22	6.1×10^{-2}	0.3	1.66×10^{-2}
S_3	3.43×10^{-2}	5.92×10^{-3}	0.12	2.2×10^{-2}	0.24	4.29×10^{-3}
S_4	2.72×10^{-3}	1.1×10^{-4}	8.16×10^{-3}	5.1×10^{-4}	2.41×10^{-3}	8×10^{-5}
S_5	1.56×10^{-3}	8.0×10^{-5}	4.48×10^{-3}	3.4×10^{-4}	1.3×10^{-4}	10^{-5}
S_6	1.2×10^{-3}	7×10^{-5}	5.4×10^{-4}	3×10^{-5}	7×10^{-5}	0
S_7	8.8×10^{-4}	3×10^{-5}	2.2×10^{-4}	2×10^{-5}	0	0

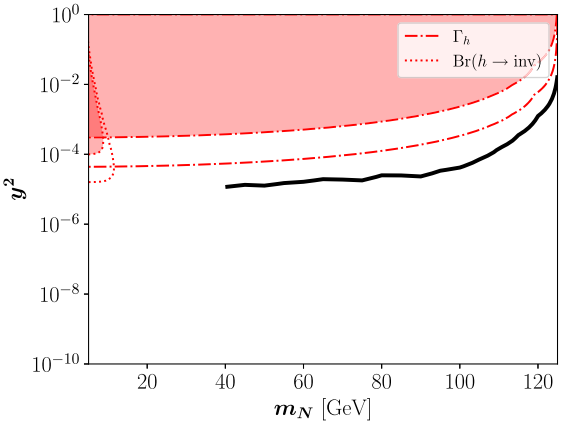

FIG. 3. Sensitivity reach of searches for a prompt decay, for $\sqrt{s} = 14$ TeV and $\mathcal{L} = 3$ ab^{-1}. The red areas are in tension with the invisible decay of the Higgs or its total decay width, whereas the red dotted and dashed dotted areas correspond to the projected sensitivity at HL-LHC.

invariant mass ($m_{j_1 j_2} > 500$ GeV). In addition, they should not be back-to-back ($\Delta\phi_{j_1 j_2} < 2.5$).

S5: Any existing third or fourth non-b jet must have $m_{j_i}^{\text{rel}} < 0.08$.

S6: A cut on the missing transverse energy is helpful in reducing the background arising from the decays of SM Higgs to two b jets. We demand $\not{E}_T > 50$ GeV.

S7: Finally, we demand a cut on the invariant mass of the two leading b-tagged jets given by $0.2m_N \leq m_{b\bar{b}} \leq 1.6m_N$. We also put a cut on the separation between the two b-tagged jets given by $\Delta R_{b\bar{b}} \leq 2.5$.

An example of the cut flow after the implementation of the above cuts for $m_N = 65$ GeV is shown in Table I.

The discovery significance is given by

$$\sigma_3 = \frac{\mathcal{N}_S}{\sqrt{\mathcal{N}_S + \mathcal{N}_B}}, \tag{4.2}$$

where σ_3 denotes the discovery significance at a luminosity of $\mathcal{L} = 3$ ab^{-1}, with $\mathcal{N}_S$ and $\mathcal{N}_B$ denoting the corresponding number of signal and background events that fulfill all previous cuts. Figure 3 shows, with a thick solid black line, the sensitivity reach of searches for a prompt decay for $\sqrt{s} = 14$ TeV with the above luminosity, in the plane $[m_N, y^2]$. The parameter space above the line could be probed at HL-LHC. In addition, the red areas are in tension with measurements of the total decay width of the Higgs or its branching ratio into invisible, whereas the dotted and dashed dotted areas correspond to the projected sensitivity at HL-LHC.

V. DISPLACED VERTICES

In this section, we focus on the case where HNLs decay in the inner tracker of ATLAS or CMS, featuring a displaced vertex. Here too, we stick to the case where the Higgs is produced through VBF to trigger on the characteristic two hard forward jets. However, as seen in Sec. IV, ggF events can also have a non-negligible contribution to the same topology requirements and hence have been included in the analysis. For the events, we use the following selection criteria:

(1) Same cuts S_1, S_3, and S_4 for the VBF hard forward jets, as described in Sec. IV.

(2) Two extra jets with a displacement of 1 mm $\leq d_{xy} \leq$ 1 m and $d_z \leq 300$ mm.

In the first attempt, we assume that there is no background. Therefore, we follow a Poisson distribution and highlight the parameter space where there are more than 3.09 expected signal events at 95% CL [130]. Figure 4 shows, with a thick solid black line, the sensitivity reach of searches for a displaced decay for $\sqrt{s} = 14$ TeV and $\mathcal{L} = 3$ ab^{-1} in the plane $[m_N, y^2]$. The rectangular shape of the sensitivity reach can be understood as follows. High values for m_N and y^2 cause prompt decays; in contrast, low values generate decays outside the detector. Finally, very small values of the Yukawa coupling cannot be explored due to lack of statistics; see Eq. (3.2). In the figure, we also overlay in red the areas that are in tension with current measurements of the total decay width of the Higgs, or its branching ratio into invisible, whereas the red dotted and dashed dotted areas correspond to the projected sensitivity at HL-LHC. Yukawa couplings as small as $y^2 \simeq \mathcal{O}(10^{-8})$ could be probed for the mass range 60 GeV $\lesssim m_N \lesssim$ 100 GeV.

The previously used background-free hypothesis could be too optimistic, since background events could come from misidentified displaced events due to detector resolution effects or from random track crossings. To have a

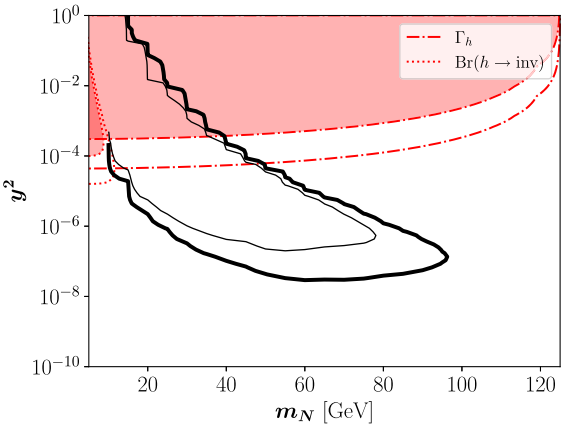

FIG. 4. Sensitivity reach of searches for a displaced decay, for $\sqrt{s} = 14$ TeV and $\mathcal{L} = 3$ ab^{-1}. The thick line corresponds to the assumption of zero background events, whereas for the thin line 65 events were assumed; see the text for further details. The red areas are in tension with the invisible decay of the Higgs or its total decay width, whereas the red dotted and dashed dotted areas correspond to the projected sensitivity at HL-LHC.

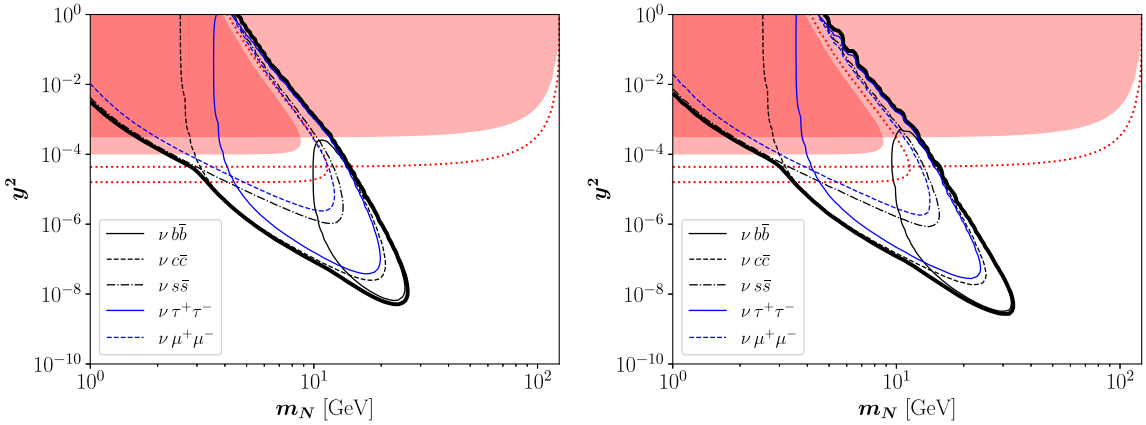

FIG. 5. The sensitivity reaches of FASER (left) and MATHUSLA (right) are represented by solid black lines, for $\sqrt{s} = 14$ TeV and $\mathcal{L} = 3$ ab^{-1}. The partial contributions of the different channels are shown with thin lines. The red areas are in tension with the invisible decay of the Higgs or its total decay width, whereas the red dotted and dashed dotted areas correspond to the projected sensitivity at HL-LHC.

rough estimate of how much the inclusion of a background could worsen the sensitivity, we follow the discussion in Refs. [68–70,76], and assume the largest possible background that is in agreement with not having observed any background event in the ATLAS analysis of Refs. [138,139]. This means up to three background events for $\mathcal{L} = 139$ fb^{-1}, which can be scaled to 65 background events for a luminosity of 3 ab^{-1}. This pessimistic scenario is shown in Fig. 4 with a thin black line. This would imply that the HL-LHC could still provide new information on HNLs that display a displaced vertex; in particular, Yukawa couplings of the order $y^2 \simeq \mathcal{O}(10^{-7})$ could be probed if 60 GeV $\lesssim m_N \lesssim$ 80 GeV. However, again we stress that a complete background analysis is needed to have more realistic LHC sensitivities.

VI. LONG-LIVED PARTICLES

Long-lived HNLs could be looked for in already approved detectors at the LHC such as FASER [92] and MoEDAL-MAPP1 [94]. They also have follow-up programs at the high-luminosity (HL) LHC: FASER-2 [93] and MoEDAL-MAPP2 [95]. Other experimental proposals include MATHUSLA [96–98], ANUBIS [99], CODEX-b [100], and more recently, FACET [101]. All of these detectors will be sensitive to particles that decay $\mathcal{O}(10)$ m to $\mathcal{O}(500)$ m away from the interaction point (IP). The large distance to the IP guarantees a very low background environment, typically assumed to be negligible. Therefore, only 3.09 events are required to define the sensitivity of the experiment at 95% CL [130].

In this section, we will consider HNLs produced by Higgs decays. The total single-Higgs boson inclusive cross section is dominated by the ggF and VBF processes, which is $\sigma \simeq 59.1$ pb at $\sqrt{s} = 14$ TeV [126,127]. We will again use a total integrated luminosity $\mathcal{L} = 3$ ab^{-1}, and focus on two detectors: FASER and MATHUSLA.

The FASER detector is located at $L = 480$ m downstream of the proton-proton IP used by the ATLAS experiment [92,93]. It is sensitive to new particles that decay in a cylindrical volume with radius $R = 10$ cm and length $\Delta = 1.5$ m. In its first phase, it will operate with integrated luminosity $\mathcal{L} = 150$ fb^{-1}. However, a second phase (FASER-2) is expected to operate with $\Delta = 10$ m, $R = 1$ m, and $\mathcal{L} = 3$ ab^{-1}, at the HL-LHC. Here, we will focus on this second phase.

Given the geometry of FASER, the probability $\mathcal{P}$ of a HNL decaying inside the detector is[4]

$$\mathcal{P} = [e^{-(L-\Delta)/d} - e^{-L/d}]\,\Theta\,[R - L\tan\theta], \tag{6.1}$$

where d is the decay length in the laboratory frame of the HNL, and θ the angle between the momentum and the beam line. This decay length takes into account the Lorentz boost factor

$$d = c\tau\beta\gamma = c\tau\frac{|\vec{p}|}{m_N}. \tag{6.2}$$

The left panel of Fig. 5 shows, with a thick solid black line, the sensitivity reach of FASER-2 to HNLs in the plane $[m_N, y^2]$. For completeness, the partial contributions of the different channels are also shown with thin lines. As expected, FASER is sensitive to masses smaller than in the cases of prompt decays and displaced vertices because a much longer decay length is required. Additionally, the red areas in the figure are in tension with measurements of the total decay width of the Higgs or its branching ratio into invisible, whereas the red dotted and dashed dotted areas

[4]We note that a code for estimating the sensitivities of long-lived particles in different detectors has recently been released [140]; here, however, we use our own implementation.

correspond to the projected sensitivity at HL-LHC. It is interesting to note that the experiment will be sensitive to unconstrained regions of the parameter space corresponding to masses between ∼3 and ∼30 GeV and couplings as low as $y^2 \simeq \mathcal{O}(10^{-8})$.

MATHUSLA [98] is a box-shaped 100 m × 100 m × 25 m far detector for the CMS interaction point. Taking the CMS IP to be located at $x = y = z = 0$, its front and depth are parallel to the beam axis, at distances $z_{\rm min} = 68$ m and $z_{\rm max} = 168$ m. Its base and cover are located at $y_{\rm min} = 60$ m and $y_{\rm max} = 85$ m, above the beam. The boundaries on the left and right sides are slightly offset, $x_{\rm min} = -42.41$ m and $x_{\rm max} = 57.59$ m. The right panel of Fig. 5 compares to the left panel, but for the case of MATHUSLA. We note that the sensitivity reach for both experiments is comparable, although MATHUSLA could probe a slightly larger parameter space and smaller Yukawa couplings $y^2 \simeq \mathcal{O}(10^{-9})$.

VII. CONCLUSIONS

The introduction of HNLs is a natural and minimal extension of the SM that can play a fundamental role in the solution of long-standing problems such as the generation of neutrino masses, the baryon asymmetry of the Universe and the dark matter. Many experimental searches have been conducted with the aim of discovering HNLs, mainly, if not exclusively, through its potential mixing with active SM neutrinos.

Alternatively, here, we have focused on a novel and complementary approach, exploiting the Yukawa interaction between HNLs and the SM Higgs boson. Even if a relation can be expected between the mixing and the Yukawa couplings, it is model dependent and therefore cannot be taken for granted. With this in mind, in this first study we have ignored potential large mixings and analyzed the reach of HL-LHC to discover HNLs through their Yukawa coupling to the SM Higgs.

In this scenario, HNLs are produced by the decay of Higgs bosons. Depending on its mass and Yukawa coupling, HNLs can decay promptly inside ATLAS or CMS detectors, feature a displaced vertex in the tracker, or even decay far away from the interaction point in far detectors such as FASER or MATHUSLA. The sensitivity reach of each of these options is presented in Figs. 3–5, respectively. To facilitate comparison, Fig. 6 summarizes in blue the combined sensitivity reach for $\sqrt{s} = 14$ TeV and $\mathcal{L} = 3$ ab^{-1}. Note that the red areas are in tension with current measurements of the total decay width of the Higgs boson or its branching ratio into invisible. In Fig. 6, we also present the projected sensitivity obtained from the invisible decay of the Higgs boson and the future measurement of the total decay width of the Higgs boson at HL-LHC [131]. HL-LHC combined with future Higgs factories have the potential to reach precision up to 1% for the branching corresponding to invisible decay of the Higgs boson and up to 1.1% for the total width of the Higgs boson [131], which roughly translates to a value of $y^2 \sim 9 \times 10^{-6}$.

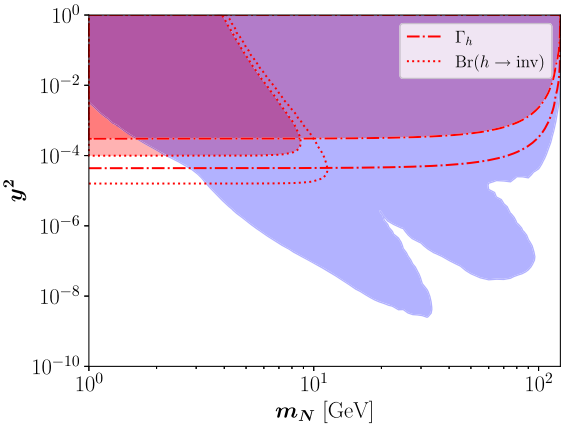

FIG. 6. The combined sensitivity reach for searches of prompt decays, displaced vertices in the tracker and decays in far detectors (FASER and MATHUSLA), for $\sqrt{s} = 14$ TeV and $\mathcal{L} = 3$ ab^{-1}, is represented in blue. The red areas are in tension with the invisible decay of the Higgs or its total decay width, whereas the red dotted and dashed dotted areas correspond to the projected sensitivity at HL-LHC.

ACKNOWLEDGMENTS

We thank Giovanna Cottin, Marco Drewes, Chee Sheng Fong, and Avelino Vicente for valuable discussions.

APPENDIX

The decoupling between the Yukawa coupling between SM neutrinos and HNL can be achieved if we allow the HNLs to be Dirac particles (ν_L, ν_R) and prevent tree-level Dirac mass terms by introducing additional symmetries. By incorporating a heavy Dirac HNL (N_L, N_R) and new complex scalar singlets with specific charges under the new symmetries such that only N_R couples to the light neutrino (ν_L) via the SM Higgs and N_L couples to ν_R via a new complex scalar singlet, we achieve two distinct Dirac masses in the neutrino-mass matrix. References [117,118] achieve this by extending the SM gauge group with a $\mathbb{Z}_4 \otimes \mathbb{Z}_2$ and a $U(1)_{B-L}$, respectively. The part of the Lagrangian for one generation of neutrinos that holds relevance in the current context can be written as

$$\mathcal{L} \supset y \bar{L}_L \tilde{H} N_R + g \bar{N}_L \chi \nu_R + M \bar{N}_L N_R, \tag{A1}$$

with $\langle H \rangle = (0, v_h/\sqrt{2})^T$, $\langle \chi \rangle = v_\chi$ and $\tilde{H} = i\tau_2 H^*$, with τ_2 the second Pauli matrix and $v_h \simeq 246$ GeV. After the Higgs (H) and the new scalar (χ) get a vev, the ensuing mass matrix can be written as

$$\mathcal{M} = \begin{pmatrix} 0 & m_1 \\ m_2 & M \end{pmatrix}, \tag{A2}$$

where $m_1 \equiv yv_h/\sqrt{2}$ and $m_2 \equiv gv_\chi$. The mass matrix can be diagonalized through $\mathcal{M}_D = P^{-1}\mathcal{M}P$, where

$$P = \begin{pmatrix} \frac{2m_1}{\sqrt{4m_1^2+(M-\sqrt{M^2+4m_1m_2})^2}} & \frac{2m_1}{\sqrt{4m_1^2+(M+\sqrt{M^2+4m_1m_2})^2}} \\ \frac{(M-\sqrt{M^2+4m_1m_2})}{\sqrt{4m_1^2+(M-\sqrt{M^2+4m_1m_2})^2}} & \frac{(M+\sqrt{M^2+4m_1m_2})}{\sqrt{4m_1^2+(M+\sqrt{M^2+4m_1m_2})^2}} \end{pmatrix} \tag{A3}$$

and the diagonal matrix with the two eigenvalues denoted by

$$\mathcal{M}_D = \begin{pmatrix} \frac{1}{2}[M-\sqrt{M^2+4m_1m_2}] & 0 \\ 0 & \frac{1}{2}[M+\sqrt{M^2+4m_1m_2}] \end{pmatrix}. \tag{A4}$$

The flavor states and mass states are related through

$$\begin{pmatrix} \bar{\nu}_L \\ \bar{N}_L \end{pmatrix} = (P^{-1})^T \begin{pmatrix} \bar{\nu}_L^m \\ \bar{N}_L^m \end{pmatrix}, \qquad \begin{pmatrix} \nu_R \\ N_R \end{pmatrix} = P \begin{pmatrix} \nu_R^m \\ N_R^m \end{pmatrix}, \tag{A5}$$

where $(\bar{\nu}_L^m\, \bar{N}_L^m)^T$ and $(\nu_R^m\, N_R^m)^T$ are the mass eigenstates. In the limit of m_2 becoming negligible, these relations become

$$\begin{pmatrix} \bar{\nu}_L \\ \bar{N}_L \end{pmatrix} = \begin{pmatrix} \bar{\nu}_L^m \\ \frac{\sqrt{m_1^2+M^2}}{M}\bar{N}_L^m - \frac{m_1}{M}\bar{\nu}_L^m \end{pmatrix}, \qquad \begin{pmatrix} \nu_R \\ N_R \end{pmatrix} = \begin{pmatrix} \nu_R^m + \frac{m_1}{\sqrt{m_1^2+M^2}}N_R^m \\ \frac{M}{\sqrt{m_1^2+M^2}}N_R^m \end{pmatrix}. \tag{A6}$$

In this limit, ν_L and N_R, which provide the Yukawa term with the Higgs, are pure states and hence do not have any mixing term. However, mixings appear for nonvanishing m_2. In the limit $m_2 \ll M$, one has

$$\begin{pmatrix} \bar{\nu}_L \\ \bar{N}_L \end{pmatrix} = \begin{pmatrix} \left[1-\frac{m_1m_2}{M^2}\right]\bar{\nu}_L^m + \frac{m_2\sqrt{m_1^2+M^2}}{M^2}\bar{N}_L^m \\ -\frac{m_1}{M}\bar{\nu}_L^m + \frac{\sqrt{m_1^2+M^2}}{M}\bar{N}_L^m \end{pmatrix}, \qquad \begin{pmatrix} \nu_R \\ N_R \end{pmatrix} = \begin{pmatrix} \left[1-\frac{m_2^2}{2M^2}\right]\nu_R^m + \frac{m_1}{\sqrt{m_1^2+M^2}}N_R^m \\ -\frac{m_2}{M}\nu_R^m + \frac{M}{\sqrt{m_1^2+M^2}}N_R^m \end{pmatrix}. \tag{A7}$$

The charged and neutral current interactions of the SM gauge bosons with the light neutrinos (ν_L) become

$$\mathcal{L}_{cc}^{\nu_L} \sim -\frac{g}{2\sqrt{2}}\left\{\left(1-\frac{m_1m_2}{M^2}\right)[(\bar{\nu}_L^m\gamma^\mu l_L)W_\mu^\dagger] + \frac{m_2\sqrt{m_1^2+M^2}}{M^2}[(\bar{N}_L^m\gamma^\mu l_L)W_\mu^\dagger] + \text{H.c.}\right\}, \tag{A8}$$

$$\begin{aligned}\mathcal{L}_{nc}^{\nu_L} \sim -\frac{e}{2\sin\theta_W\cos\theta_W}\Bigg\{&\left(1-\frac{2m_1m_2}{M^2}\right)[(\bar{\nu}_L^m\gamma^\mu\nu_L^m)Z_\mu] \\ &+ \frac{2m_2\sqrt{m_1^2+M^2}}{M^2}[(\bar{\nu}_L^m\gamma^\mu N_L^m)Z_\mu] + \frac{m_2^2(m_1^2+M^2)}{M^4}[(\bar{N}_L^m\gamma^\mu N_L^m)Z_\mu]\Bigg\}.\end{aligned} \tag{A9}$$

Similarly, the Yukawa term with the physical SM Higgs boson (h) can now be written as

$$\begin{aligned}\mathcal{L}_{Yuk}^{\nu_L} \sim \frac{y}{\sqrt{2}}\Bigg\{&\left(1-\frac{m_1m_2}{M^2}\right)\left(\frac{M}{\sqrt{m_1^2+M^2}}\right)[\bar{\nu}_L^m N_R^m h] - \left(\frac{m_2}{M}\right)[\bar{\nu}_L^m\nu_R^m h] \\ &- \left(\frac{m_2^2\sqrt{m_1^2+M^2}}{M^3}\right)[\bar{N}_L^m\nu_R^m h] + \left(\frac{m_2}{M}\right)[\bar{N}_L^m N_R^m h]\Bigg\}.\end{aligned} \tag{A10}$$

It is clear from Eqs. (A8)–(A10) that the production and decay of N_R^m is only possible through the Yukawa interaction with h and ν_L^m at tree level, while the SM gauge-boson interactions through mixing do not play a role in it (or in other words, the mixing is precisely zero). For small m_2 values, only the first term of Eq. (A10) will contribute to the phenomenology related to N_R. In contrast, N_L couples to the gauge bosons through mixing and can have potentially higher production and decay rates compared to the Yukawa interactions.

[1] ATLAS Collaboration, Observation of a new particle in the search for the Standard Model Higgs boson with the ATLAS detector at the LHC, Phys. Lett. B **716**, 1 (2012).

[2] CMS Collaboration, Observation of a new boson at a mass of 125 GeV with the CMS experiment at the LHC, Phys. Lett. B **716**, 30 (2012).

[3] D. P. Barber *et al.*, Discovery of three jet events and a test of quantum chromodynamics at PETRA energies, Phys. Rev. Lett. **43**, 830 (1979).

[4] UA1 Collaboration, Experimental observation of isolated large transverse energy electrons with associated missing energy at $\sqrt{s} = 540$ GeV, Phys. Lett. **122B**, 103 (1983).

[5] E598 Collaboration, Experimental observation of a heavy particle J, Phys. Rev. Lett. **33**, 1404 (1974).

[6] D. P. Roy and S. U. Sankar, B_d^0 - $\bar{B}_d^0$ mixing as the evidence for the existence of the top quark, Phys. Lett. B **243**, 296 (1990).

[7] CDF Collaboration, Evidence for top quark production in $\bar{p}p$ collisions at $\sqrt{s} = 1.8$ TeV, Phys. Rev. Lett. **73**, 225 (1994).

[8] K. N. Abazajian *et al.*, Light sterile neutrinos: A white paper, arXiv:1204.5379.

[9] A. M. Abdullahi *et al.*, The present and future status of heavy neutral leptons, J. Phys. G **50**, 020501 (2023).

[10] P. Minkowski, $\mu \to e\gamma$ at a rate of one out of 10^9 muon decays?, Phys. Lett. **67B**, 421 (1977).

[11] M. Gell-Mann, P. Ramond, and R. Slansky, Complex spinors and unified theories, Conf. Proc. C **790927**, 315 (1979), https://inspirehep.net/literature/9686.

[12] T. Yanagida, Horizontal gauge symmetry and masses of neutrinos, Conf. Proc. C **7902131**, 95 (1979), https://neutrino.kek.jp/seesaw/KEK-79-18-Yanagida.pdf.

[13] R. N. Mohapatra and G. Senjanovic, Neutrino mass and spontaneous parity nonconservation, Phys. Rev. Lett. **44**, 912 (1980).

[14] S. L. Glashow, The future of elementary particle physics, NATO Sci. Ser. B **61**, 687 (1980).

[15] J. Schechter and J. W. F. Valle, Neutrino masses in $SU(2) \times U(1)$ theories, Phys. Rev. D **22**, 2227 (1980).

[16] J. Schechter and J. W. F. Valle, Neutrino decay and spontaneous violation of lepton number, Phys. Rev. D **25**, 774 (1982).

[17] R. Foot, H. Lew, X. G. He, and G. C. Joshi, Seesaw neutrino masses induced by a triplet of leptons, Z. Phys. C **44**, 441 (1989).

[18] E. Ma, Pathways to naturally small neutrino masses, Phys. Rev. Lett. **81**, 1171 (1998).

[19] D. Choudhury, K. Deka, T. Mandal, and S. Sadhukhan, Neutrino and Z' phenomenology in an anomaly-free $U(1)$ extension: Role of higher-dimensional operators, J. High Energy Phys. 06 (2020) 111.

[20] M. Fukugita and T. Yanagida, Baryogenesis without grand unification, Phys. Lett. B **174**, 45 (1986).

[21] E. K. Akhmedov, V. A. Rubakov, and A. Y. Smirnov, Baryogenesis via neutrino oscillations, Phys. Rev. Lett. **81**, 1359 (1998).

[22] T. Asaka and M. Shaposhnikov, The νMSM, dark matter and baryon asymmetry of the universe, Phys. Lett. B **620**, 17 (2005).

[23] S. Davidson, E. Nardi, and Y. Nir, Leptogenesis, Phys. Rep. **466**, 105 (2008).

[24] T. Hambye and D. Teresi, Higgs doublet decay as the origin of the baryon asymmetry, Phys. Rev. Lett. **117**, 091801 (2016).

[25] K. Deka, T. Mandal, A. Mukherjee, and S. Sadhukhan, Leptogenesis in an anomaly-free U(1) extension with higher-dimensional operators, Nucl. Phys. **B991**, 116213 (2023).

[26] S. Dodelson and L. M. Widrow, Sterile-neutrinos as dark matter, Phys. Rev. Lett. **72**, 17 (1994).

[27] X.-D. Shi and G. M. Fuller, A new dark matter candidate: Nonthermal sterile neutrinos, Phys. Rev. Lett. **82**, 2832 (1999).

[28] K. Abazajian, G. M. Fuller, and M. Patel, Sterile neutrino hot, warm, and cold dark matter, Phys. Rev. D **64**, 023501 (2001).

[29] T. Asaka, S. Blanchet, and M. Shaposhnikov, The νMSM, dark matter and neutrino masses, Phys. Lett. B **631**, 151 (2005).

[30] DELPHI Collaboration, Search for neutral heavy leptons produced in Z decays, Z. Phys. C **74**, 57 (1997).

[31] ATLAS Collaboration, Inclusive search for same-sign dilepton signatures in pp collisions at $\sqrt{s} = 7$ TeV with the ATLAS detector, J. High Energy Phys. 10 (2011) 107.

[32] CMS Collaboration, Search for heavy Majorana neutrinos in $\mu^\pm\mu^\pm +$ jets and $e^\pm e^\pm +$ jets events in pp collisions at $\sqrt{s} = 7$ TeV, Phys. Lett. B **717**, 109 (2012).

[33] CMS Collaboration, Search for heavy Majorana neutrinos in $\mu^\pm\mu^\pm +$ jets events in proton-proton collisions at $\sqrt{s} = 8$ TeV, Phys. Lett. B **748**, 144 (2015).

[34] ATLAS Collaboration, Search for heavy Majorana neutrinos with the ATLAS detector in pp collisions at $\sqrt{s} = 8$ TeV, J. High Energy Phys. 07 (2015) 162.

[35] CMS Collaboration, Search for heavy Majorana neutrinos in ee+ jets and e μ+ jets events in proton-proton collisions at $\sqrt{s} = 8$ TeV, J. High Energy Phys. 04 (2016) 169.
[36] CMS Collaboration, Search for heavy neutral leptons in events with three charged leptons in proton-proton collisions at $\sqrt{s} = 13$ TeV, Phys. Rev. Lett. **120**, 221801 (2018).
[37] F. del Águila, J. A. Aguilar-Saavedra, and R. Pittau, Heavy neutrino signals at large hadron colliders, J. High Energy Phys. 10 (2007) 047.
[38] F. del Águila and J. A. Aguilar-Saavedra, Distinguishing seesaw models at LHC with multi-lepton signals, Nucl. Phys. **B813**, 22 (2009).
[39] F. del Águila and J. A. Aguilar-Saavedra, Electroweak scale seesaw and heavy Dirac neutrino signals at LHC, Phys. Lett. B **672**, 158 (2009).
[40] A. Atre, T. Han, S. Pascoli, and B. Zhang, The search for heavy Majorana neutrinos, J. High Energy Phys. 05 (2009) 030.
[41] P. S. Bhupal Dev, R. Franceschini, and R. N. Mohapatra, Bounds on TeV seesaw models from LHC Higgs data, Phys. Rev. D **86**, 093010 (2012).
[42] P. S. B. Dev, A. Pilaftsis, and U.-k. Yang, New production mechanism for heavy neutrinos at the LHC, Phys. Rev. Lett. **112**, 081801 (2014).
[43] A. Das, P. S. Bhupal Dev, and N. Okada, Direct bounds on electroweak scale pseudo-Dirac neutrinos from $\sqrt{s} =$ 8 TeV LHC data, Phys. Lett. B **735**, 364 (2014).
[44] D. Alva, T. Han, and R. Ruiz, Heavy Majorana neutrinos from $W\gamma$ fusion at hadron colliders, J. High Energy Phys. 02 (2015) 072.
[45] F. F. Deppisch, P. S. Bhupal Dev, and A. Pilaftsis, Neutrinos and collider physics, New J. Phys. **17**, 075019 (2015).
[46] S. Banerjee, P. S. B. Dev, A. Ibarra, T. Mandal, and M. Mitra, Prospects of heavy neutrino searches at future lepton colliders, Phys. Rev. D **92**, 075002 (2015).
[47] E. Arganda, M. J. Herrero, X. Marcano, and C. Weiland, Exotic $\mu\tau jj$ events from heavy ISS neutrinos at the LHC, Phys. Lett. B **752**, 46 (2016).
[48] A. Das and N. Okada, Improved bounds on the heavy neutrino productions at the LHC, Phys. Rev. D **93**, 033003 (2016).
[49] C. Degrande, O. Mattelaer, R. Ruiz, and J. Turner, Fully-automated precision predictions for heavy neutrino production mechanisms at hadron colliders, Phys. Rev. D **94**, 053002 (2016).
[50] M. Mitra, R. Ruiz, D. J. Scott, and M. Spannowsky, Neutrino jets from high-mass W_R gauge bosons in TeV-scale left-right symmetric models, Phys. Rev. D **94**, 095016 (2016).
[51] A. Das, P. S. B. Dev, and C. S. Kim, Constraining sterile neutrinos from precision Higgs data, Phys. Rev. D **95**, 115013 (2017).
[52] A. Das, Y. Gao, and T. Kamon, Heavy neutrino search via semileptonic Higgs decay at the LHC, Eur. Phys. J. C **79**, 424 (2019).
[53] R. Ruiz, M. Spannowsky, and P. Waite, Heavy neutrinos from gluon fusion, Phys. Rev. D **96**, 055042 (2017).
[54] Y. Cai, T. Han, T. Li, and R. Ruiz, Lepton number violation: Seesaw models and their collider tests, Front. Phys. **6**, 40 (2018).
[55] E. Accomando, L. Delle Rose, S. Moretti, E. Olaiya, and C. H. Shepherd-Themistocleous, Extra Higgs boson and Z' as portals to signatures of heavy neutrinos at the LHC, J. High Energy Phys. 02 (2018) 109.
[56] M. Drewes, J. Hajer, J. Klaric, and G. Lanfranchi, NA62 sensitivity to heavy neutral leptons in the low scale seesaw model, J. High Energy Phys. 07 (2018) 105.
[57] S. Pascoli, R. Ruiz, and C. Weiland, Safe jet vetoes, Phys. Lett. B **786**, 106 (2018).
[58] A. Bhaskar, Y. Chaurasia, K. Deka, T. Mandal, S. Mitra, and A. Mukherjee, Right-handed neutrino pair production via second-generation leptoquarks, Phys. Lett. B **843**, 138039 (2023).
[59] M. Gronau, C. N. Leung, and J. L. Rosner, Extending limits on neutral heavy leptons, Phys. Rev. D **29**, 2539 (1984).
[60] M. Nemevšek, F. Nesti, G. Senjanović, and Y. Zhang, First limits on left-right symmetry scale from LHC data, Phys. Rev. D **83**, 115014 (2011).
[61] J. C. Helo, M. Hirsch, and S. Kovalenko, Heavy neutrino searches at the LHC with displaced vertices, Phys. Rev. D **89**, 073005 (2014).
[62] E. Izaguirre and B. Shuve, Multilepton and lepton jet probes of sub-weak-scale right-handed neutrinos, Phys. Rev. D **91**, 093010 (2015).
[63] S. Dube, D. Gadkari, and A. M. Thalapillil, Lepton-jets and low-mass sterile neutrinos at hadron colliders, Phys. Rev. D **96**, 055031 (2017).
[64] G. Cottin, J. C. Helo, and M. Hirsch, Searches for light sterile neutrinos with multitrack displaced vertices, Phys. Rev. D **97**, 055025 (2018).
[65] G. Cottin, J. C. Helo, and M. Hirsch, Displaced vertices as probes of sterile neutrino mixing at the LHC, Phys. Rev. D **98**, 035012 (2018).
[66] C. O. Dib, C. S. Kim, N. A. Neill, and X.-B. Yuan, Search for sterile neutrinos decaying into pions at the LHC, Phys. Rev. D **97**, 035022 (2018).
[67] M. Nemevšek, F. Nesti, and G. Popara, Keung-Senjanović process at the LHC: From lepton number violation to displaced vertices to invisible decays, Phys. Rev. D **97**, 115018 (2018).
[68] A. Abada, N. Bernal, M. Losada, and X. Marcano, Inclusive displaced vertex searches for heavy neutral leptons at the LHC, J. High Energy Phys. 01 (2019) 093.
[69] X. Marcano, Heavy neutral leptons and displaced vertices at LHC, in *53rd Rencontres de Moriond on Electroweak Interactions and Unified Theories* (2018), pp. 311–316, arXiv:1808.04705.
[70] A. Abada, N. Bernal, M. Losada, and X. Marcano, Searching for heavy neutral leptons with displaced vertices at the LHC, in *38th International Symposium on Physics in Collision* (2018), arXiv:1812.01720.
[71] A. Maiezza, M. Nemevšek, and F. Nesti, Lepton number violation in Higgs decay at LHC, Phys. Rev. Lett. **115**, 081802 (2015).
[72] A. M. Gago, P. Hernández, J. Jones-Pérez, M. Losada, and A. Moreno Briceño, Probing the type I Seesaw mechanism with displaced vertices at the LHC, Eur. Phys. J. C **75**, 470 (2015).

[73] E. Accomando, L. Delle Rose, S. Moretti, E. Olaiya, and C. H. Shepherd-Themistocleous, Novel SM-like Higgs decay into displaced heavy neutrino pairs in $U(1)'$ models, J. High Energy Phys. 04 (2017) 081.
[74] M. Nemevšek, F. Nesti, and J. C. Vásquez, Majorana Higgses at colliders, J. High Energy Phys. 04 (2017) 114.
[75] A. Caputo, P. Hernández, J. López-Pavón, and J. Salvado, The seesaw portal in testable models of neutrino masses, J. High Energy Phys. 06 (2017) 112.
[76] F. F. Deppisch, W. Liu, and M. Mitra, Long-lived heavy neutrinos from Higgs decays, J. High Energy Phys. 08 (2018) 181.
[77] J. Liu, Z. Liu, and L.-T. Wang, Enhancing long-lived particles searches at the LHC with precision timing information, Phys. Rev. Lett. **122**, 131801 (2019).
[78] S. Antusch, E. Cazzato, and O. Fischer, Sterile neutrino searches via displaced vertices at LHCb, Phys. Lett. B **774**, 114 (2017).
[79] LBNE Collaboration, The long-baseline neutrino experiment: Exploring fundamental symmetries of the universe, arXiv:1307.7335.
[80] J. Y. Günther, J. de Vries, H. K. Dreiner, Z. S. Wang, and G. Zhou, Long-lived neutral fermions at the DUNE near detector, J. High Energy Phys. 01 (2024) 108.
[81] P. Coloma, P. A. N. Machado, I. Martínez-Soler, and I. M. Shoemaker, Double-cascade events from new physics in Icecube, Phys. Rev. Lett. **119**, 201804 (2017).
[82] FCC-ee study Team, Search for heavy right handed neutrinos at the FCC-ee, Nucl. Part. Phys. Proc. **273–275**, 1883 (2016).
[83] S. Antusch, E. Cazzato, and O. Fischer, Displaced vertex searches for sterile neutrinos at future lepton colliders, J. High Energy Phys. 12 (2016) 007.
[84] S. Alekhin *et al.*, A facility to search for hidden particles at the CERN SPS: The SHiP physics case, Rep. Prog. Phys. **79**, 124201 (2016).
[85] SHiP Collaboration, A facility to search for hidden particles (SHiP) at the CERN SPS, arXiv:1504.04956.
[86] W. Bonivento *et al.*, Proposal to search for heavy neutral leptons at the SPS, arXiv:1310.1762.
[87] CMS Collaboration, Search for heavy Majorana neutrinos in $\mu^{\pm}\mu^{\pm} + \text{jets}$ events in proton-proton collisions at $\sqrt{s} = 8$ TeV, Phys. Lett. B **748**, 144 (2015).
[88] CMS Collaboration, Search for heavy neutral leptons in events with three charged leptons in proton-proton collisions at $\sqrt{s} = 13$ TeV, Phys. Rev. Lett. **120**, 221801 (2018).
[89] ATLAS Collaboration, Search for heavy neutral leptons in decays of W bosons produced in 13 TeV pp collisions using prompt and displaced signatures with the ATLAS detector, J. High Energy Phys. 10 (2019) 265.
[90] CMS Collaboration, Search for long-lived heavy neutral leptons with displaced vertices in proton-proton collisions at $\sqrt{s} = 13$ TeV, J. High Energy Phys. 07 (2022) 081.
[91] ATLAS Collaboration, Search for heavy neutral leptons in decays of W bosons using a dilepton displaced vertex in s = 13 TeV pp collisions with the ATLAS detector, Phys. Rev. Lett. **131**, 061803 (2023).
[92] J. L. Feng, I. Galon, F. Kling, and S. Trojanowski, ForwArd Search ExpeRiment at the LHC, Phys. Rev. D **97**, 035001 (2018).
[93] FASER Collaboration, FASER's physics reach for long-lived particles, Phys. Rev. D **99**, 095011 (2019).
[94] J. L. Pinfold, The MoEDAL experiment at the LHC—A progress report, Universe **5**, 47 (2019).
[95] J. L. Pinfold, The MoEDAL experiment: A new light on the high-energy frontier, Phil. Trans. R. Soc. A **377**, 20190382 (2019).
[96] J. P. Chou, D. Curtin, and H. J. Lubatti, New detectors to explore the lifetime frontier, Phys. Lett. B **767**, 29 (2017).
[97] D. Curtin *et al.*, Long-lived particles at the energy frontier: The MATHUSLA physics case, Rep. Prog. Phys. **82**, 116201 (2019).
[98] MATHUSLA Collaboration, An update to the letter of intent for MATHUSLA: Search for long-lived particles at the HL-LHC, arXiv:2009.01693.
[99] M. Bauer, O. Brandt, L. Lee, and C. Ohm, ANUBIS: Proposal to search for long-lived neutral particles in CERN service shafts, arXiv:1909.13022.
[100] V. V. Gligorov, S. Knapen, M. Papucci, and D. J. Robinson, Searching for long-lived particles: A compact detector for exotics at LHCb, Phys. Rev. D **97**, 015023 (2018).
[101] S. Cerci *et al.*, FACET: A new long-lived particle detector in the very forward region of the CMS experiment, J. High Energy Phys. 06 (2022) 110.
[102] A. Caputo, P. Hernández, M. Kekic, J. López-Pavón, and J. Salvado, The seesaw path to leptonic CP violation, Eur. Phys. J. C **77**, 258 (2017).
[103] S. Jana, N. Okada, and D. Raut, Displaced vertex signature of type-I seesaw model, Phys. Rev. D **98**, 035023 (2018).
[104] F. Kling and S. Trojanowski, Heavy neutral leptons at FASER, Phys. Rev. D **97**, 095016 (2018).
[105] J. C. Helo, M. Hirsch, and Z. S. Wang, Heavy neutral fermions at the high-luminosity LHC, J. High Energy Phys. 07 (2018) 056.
[106] D. Dercks, H. K. Dreiner, M. Hirsch, and Z. S. Wang, Long-lived fermions at AL3X, Phys. Rev. D **99**, 055020 (2019).
[107] F. Deppisch, S. Kulkarni, and W. Liu, Heavy neutrino production via Z' at the lifetime frontier, Phys. Rev. D **100**, 035005 (2019).
[108] M. Frank, M. de Montigny, P.-P. A. Ouimet, J. Pinfold, A. Shaa, and M. Staelens, Searching for heavy neutrinos with the MoEDAL-MAPP detector at the LHC, Phys. Lett. B **802**, 135204 (2020).
[109] M. Hirsch and Z. S. Wang, Heavy neutral leptons at ANUBIS, Phys. Rev. D **101**, 055034 (2020).
[110] J. Li, W. Liu, and H. Sun, Z' mediated right-handed neutrinos from meson decays at the FASER, Phys. Rev. D **109**, 035022 (2024).
[111] F. F. Deppisch, S. Kulkarni, and W. Liu, Sterile neutrinos at MAPP in the B-L model, arXiv:2311.01719.
[112] I. Esteban, M. C. González-García, M. Maltoni, T. Schwetz, and A. Zhou, The fate of hints: Updated global analysis of three-flavor neutrino oscillations, J. High Energy Phys. 09 (2020) 178.

[113] P. F. de Salas, D. V. Forero, S. Gariazzo, P. Martínez-Miravé, O. Mena, C. A. Ternes, M. Tórtola, and J. W. F. Valle, 2020 global reassessment of the neutrino oscillation picture, J. High Energy Phys. 02 (2021) 071.
[114] KATRIN Collaboration, Direct neutrino-mass measurement with sub-electronvolt sensitivity, Nat. Phys. **18**, 160 (2022).
[115] A. G. Dias, C. A. de S. Pires, P. S. Rodrigues da Silva, and A. Sampieri, A simple realization of the inverse seesaw mechanism, Phys. Rev. D **86**, 035007 (2012).
[116] S. Fraser, E. Ma, and O. Popov, Scotogenic inverse seesaw model of neutrino mass, Phys. Lett. B **737**, 280 (2014).
[117] E. Ma and R. Srivastava, Dirac or inverse seesaw neutrino masses with $B-L$ gauge symmetry and S_3 flavor symmetry, Phys. Lett. B **741**, 217 (2015).
[118] S. Centelles Chuliá, E. Ma, R. Srivastava, and J. W. F. Valle, Dirac neutrinos and dark matter stability from lepton quarticity, Phys. Lett. B **767**, 209 (2017).
[119] K. Bondarenko, A. Boyarsky, D. Gorbunov, and O. Ruchayskiy, Phenomenology of GeV-scale heavy neutral leptons, J. High Energy Phys. 11 (2018) 032.
[120] C. Degrande, C. Duhr, B. Fuks, D. Grellscheid, O. Mattelaer, and T. Reiter, UFO—The universal FeynRules output, Comput. Phys. Commun. **183**, 1201 (2012).
[121] A. Alloul, N. D. Christensen, C. Degrande, C. Duhr, and B. Fuks, FeynRules 2.0—A complete toolbox for tree-level phenomenology, Comput. Phys. Commun. **185**, 2250 (2014).
[122] J. Alwall, R. Frederix, S. Frixione, V. Hirschi, F. Maltoni, O. Mattelaer *et al.*, The automated computation of tree-level and next-to-leading order differential cross sections, and their matching to parton shower simulations, J. High Energy Phys. 07 (2014) 079.
[123] R. Frederix, S. Frixione, V. Hirschi, D. Pagani, H. S. Shao, and M. Zaro, The automation of next-to-leading order electroweak calculations, J. High Energy Phys. 07 (2018) 185.
[124] C. Bierlich *et al.*, A comprehensive guide to the physics and usage of PYTHIA 8.3, SciPost Phys. Codebases **2022**, 8 (2022).
[125] DELPHES 3 Collaboration, DELPHES 3, A modular framework for fast simulation of a generic collider experiment, J. High Energy Phys. 02 (2014) 057.
[126] https://twiki.cern.ch/twiki/bin/view/LHCPhysics/LHCHWGGGF_RUN2.
[127] https://twiki.cern.ch/twiki/bin/view/LHCPhysics/LHCHWGVBF.
[128] A. Djouadi, The anatomy of electro-weak symmetry breaking. I: The Higgs boson in the standard model, Phys. Rep. **457**, 1 (2008).
[129] LHC Higgs Cross Section Working Group, *Handbook of LHC Higgs Cross Sections: 4. Deciphering the Nature of the Higgs Sector* (CERN, Geneva, 2017).
[130] Particle Data Group, Review of particle physics, Prog. Theor. Exp. Phys. **2022**, 083C01 (2022).
[131] J. de Blas, J. Gu, and Z. Liu, Higgs boson precision measurements at a 125 GeV muon collider, Phys. Rev. D **106**, 073007 (2022).
[132] ATLAS Collaboration, Combination of searches for invisible decays of the Higgs boson using 139 fb^{-1} of proton-proton collision data at $\sqrt{s}=13$ TeV collected with the ATLAS experiment, Phys. Lett. B **842**, 137963 (2023).
[133] CMS Collaboration, A search for decays of the Higgs boson to invisible particles in events with a $t\bar{t}$ quark pair or a vector boson in proton-proton collisions at $\sqrt{s}=13$TeV, Eur. Phys. J. C **83**, 933 (2023).
[134] R. K. Ellis *et al.*, Physics briefing book: Input for the European strategy for particle physics update 2020, arXiv:1910.11775.
[135] ATLAS Collaboration, ATLAS muon spectrometer: Technical design report, Report No. CERN-LHCC-97-22, ATLAS-TDR-10, CERN, 1997, https://inspirehep.net/literature/455675.
[136] C. Muselli, M. Bonvini, S. Forte, S. Marzani, and G. Ridolfi, Top quark pair production beyond NNLO, J. High Energy Phys. 08 (2015) 076.
[137] ATLAS Collaboration, Measurement of the inclusive and dijet cross-sections of b-jets in pp collisions at $\sqrt{s}=7$ TeV with the ATLAS detector, Eur. Phys. J. C **71**, 1846 (2011).
[138] ATLAS Collaboration, Search for neutral long-lived particles in pp collisions at $\sqrt{s}=13$ TeV that decay into displaced hadronic jets in the ATLAS calorimeter, J. High Energy Phys. 06 (2022) 005.
[139] ATLAS Collaboration, Search for long-lived, massive particles in events with displaced vertices and multiple jets in pp collisions at $\sqrt{s}=13$ TeV with the ATLAS detector, J. High Energy Phys. 06 (2023) 200.
[140] F. Domingo, J. Günther, J. S. Kim, and Z. S. Wang, A C++ program for estimating detector sensitivities to long-lived particles: Displaced decay counter, Eur. Phys. J. C **84**, 642 (2024).